IEEE Photonics Journal
An IEEE Photonics Society Publication

Open Access

Zero Crosstalk Regime Direct Modulation of Mutually Coupled Nanolasers

Volume 9, Number 4, August 2017

Hong Han
K. Alan Shore, ***Senior Member, IEEE***

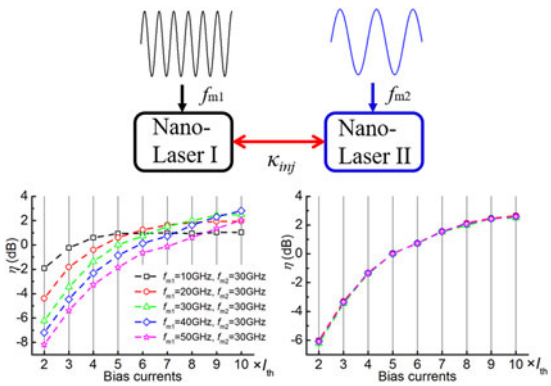

DOI: 10.1109/JPHOT.2017.2705433
1943-0655

IEEE photonics SOCIETY

IEEE

Zero Crosstalk Regime Direct Modulation of Mutually Coupled Nanolasers

Hong Han[1,2] **and K. Alan Shore,**[2] ***Senior Member, IEEE***

[1]Key Laboratory of Advanced Transducers and Intelligent Control System, Ministry of Education, College of Physics and Optoelectronics, Taiyuan University of Technology, Taiyuan 030024, China
[2]School of Electronic Engineering, Bangor University, Bangor LL57 1UT, U.K.

DOI:10.1109/JPHOT.2017.2705433

Manuscript received May 4, 2017; accepted May 12, 2017. Date of publication July 20, 2017; date of current version August 17, 2017. This work was supported in part by the Sêr Cymru National Research Network in Advanced Engineering and Materials, in part by the International Science & Technology Cooperation Program of China under Grant 2014DFA50870, in part by the National Natural Science Foundation of China under Grants 61527819, 61475111, and 61601319, in part by the Natural Science Foundation of Shanxi Province (201601D202043), and in part by the Outstanding Innovative Teams of Higher Learning Institutions of Shanxi. Corresponding author: H. Han (e-mail: hanhong@tyut.edu.cn).

Abstract: The modulation properties of dually modulated mutually coupled nanolasers have been analysed using rate equations which include the Purcell cavity-enhanced spontaneous emission factor F and the spontaneous emission coupling factor β. Specific attention is given to zero crosstalk operating regimes where the responses of the nanolasers are independent. Such regimes may provide either bidirectional isolation where both nanolasers operate independently or unidirectional-isolation where one nanolaser is immune to the other nanolaser but not vice versa. Access to the bidirectional isolation zero-crosstalk regime is, in general, enabled by strong driving or large modulation depth of the nanolasers. Conversely, strong injection coupling and low modulation depth lead to the unidirectional isolation regime. The modulation responses of the nanolasers in both bidirectional and unidirectional isolated zero crosstalk regimes are presented. The availability of bidirectional-isolated zero crosstalk regimes is seen to offer opportunities for exploitation in photonic integrated circuits.

Index Terms: Mutually-coupled semiconductor lasers, nanolasers, modulation response, modulation bandwidth.

1. Introduction

Mutually coupled lasers have been investigated for many decades [1]. Activity on mutually coupled semiconductor lasers also has long antecedents [2], [3] with significant effort having been given to identifying regimes of synchronization and instabilities [4]–[7]. Besides in-phase desynchronization, out-of-phase desynchronized was found as the delay time increased [8]. Detailed characterisation of the stable states of mutually-coupled lasers separated by short distances were investigated recently [9]. Optical injection is well-known as a means for enhancing the modulation bandwidth of semiconductor lasers [10] and in recent work modulation bandwidth enhancement in mutually-coupled monolithically integrated laser diodes has been reported [11]. Semiconductor nano-lasers [12], [13] are of interest not least for their potential for inclusion in photonic integrated circuits [14]. Fabricating nano-lasers is rather challenging and, as far as we are aware, no experimental studies of their dynamical properties have been published. In this context, it is considered appropriate to

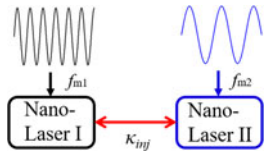

Fig. 1. Schematic diagram of modulated mutually-coupled semiconductor nano-lasers.

explore nano-laser dynamics using a generic model rather than limiting the analysis to any specific nano-laser structure. It is foreseen that such analysis may offer perspectives for future experimental exploration of nano-lasers as they become available.

In early work, the impact of Purcell enhanced spontaneous emission on the modulation performance of nano-LEDs [15] and nano-lasers [16] was examined. In addition to [17]–[20] a number of recent investigations of the dynamical performance of nanolasers have been undertaken. The behaviour of optically pumped nanolasers has been studied including the role of the spontaneous emission factor, β, in achieving single mode operation of nanolasers [16]. Ding *et al*. explored how the dynamics of electrically pumped nanolasers are impacted by F and β [21]. Marconi *et al*. investigated the universal properties in arrays of optically coupled semiconductor micro and nanocavities, the energy transfer between in-phase and out-of-phase was found for $\beta = 0.2$ [22]. Theoretical work has also been reported on the control of dynamical instability in such lasers [23].

Previous investigations of the influence of F and β shows that modulation bandwidth of up to 60 GHz can be achieved for metal clad nano-lasers [24]. In later work on the effect of optical injection in nanolasers, it has been identified the modulation bandwidth of nanolaser can approach 90 GHz [25]. For quantum-dot nanolaser system, the influence of F and β on the field amplitude and the inversion are presented using a Bloch equation model which predicts the availability of a 300 GHz modulation bandwidth [26].

In the present work, we theoretically investigate the modulation response of dually modulated mutually-coupled nano-lasers. Conditions are identified for achieving enhanced modulation bandwidth in nano-lasers subject to direct current modulation at different modulation frequencies.

2. Nano-laser Dynamics

A schematic diagram of modulated mutually coupled nano-lasers is shown in Fig. 1. This system is modelled using modified forms of rate equations which incorporate the Purcell enhanced spontaneous emission factor, F and spontaneous emission coupling factor, β which are included as shown in [17], [27].

Apart from the laser dimensions, the distinguishing features of nano-lasers as compared to conventional semiconductor lasers are the Purcell cavity-enhanced spontaneous emission factor F and the enhanced spontaneous emission coupling factor β. Enhanced spontaneous emission, coupled with reduced laser threshold current, can lead to a reduction of the laser turn-on delay. Strong damping will give rise to a long tail in the switch-off dynamics of the laser and hence will compromise both analogue and digital direct current modulation of the laser [28]. It is underlined that the Purcell factor and the spontaneous emission coupling factor impact the spontaneous emission rate as shown in (1) and (2) below [29]. Specifically it is pointed out that for Purcell factors greater than unity an effective reduction in the carrier lifetime will result. Similarly an increase of the spontaneous emission coupling factor towards unity also causes an effective reduction of the carrier lifetime. In contrast, the phase (3) is dependent on the laser gain and hence is not affected by the enhanced spontaneous emission.

$$\frac{dS_{I,II}(t)}{dt} = \Gamma\left[\frac{F\beta N_{I,II}(t)}{\tau_n} + G_n\left(N_{I,II}(t) - N_{th}\right)S_{I,II}(t)\right] + 2\frac{\kappa_{inj}}{\tau_{in}}\sqrt{S_{I,II}(t)S_{II,I}(t-\tau_{inj})}\cos(\theta_{I,II}(t)) \quad (1)$$

$$\frac{dN_{\mathrm{I,II}}(t)}{dt} = \frac{I_{\mathrm{I,II}}}{eV_b} - \frac{N_{\mathrm{I,II}}(t)}{\tau_n}\left(F\beta + (1-\beta)\right) - G_n\left(N_{\mathrm{I,II}}(t) - N_0\right) S_{\mathrm{I,II}}(t) \quad (2)$$

$$\frac{d\phi_{\mathrm{I,II}}(t)}{dt} = \frac{\alpha}{2}\Gamma G_n\left(N_{\mathrm{I,II}}(t) - N_{\mathrm{th}}\right) \pm \Delta\omega - \frac{\kappa_{\mathrm{inj}}}{\tau_{\mathrm{in}}}\sqrt{\frac{S_{\mathrm{II,I}}(t-\tau_{\mathrm{inj}})}{S_{\mathrm{I,II}}(t)}}\sin(\theta_{\mathrm{I,II}}(t)) \quad (3)$$

$$\theta_{\mathrm{I,II}}(t) = \pm\Delta\omega t + \omega_{\mathrm{II,I}}\tau_{\mathrm{inj}} + \phi_{\mathrm{I,II}}(t) - \phi_{\mathrm{II,I}}(t-\tau_{\mathrm{inj}}) \quad (4)$$

$$I_{\mathrm{I,II}}(t) = I_{dc}\left(1 + h_m \sin\left(2\pi f_{m1,m2} t\right)\right) \quad (5)$$

In the rate equations including the modulation, the subscripts 'I' and 'II' represent laser I and laser II respectively. $S(t)$ is the photon density and $N(t)$ is the carrier density, $\theta(t)$ is the phase of the laser, $\theta(t)$is the phase of injection laser. Γ is the confinement factor; τ_n and τ_p are the radiative carrier lifetime and photon lifetime respectively. G_n is the differential gain that takes into account the effect of group velocity, N_o is the transparency carrier density, ϵ is the gain saturation factor and α is the linewidth enhancement factor. $I_{\mathrm{dc}} = jI_{\mathrm{th}}$ is the dc bias current, where j is the normalized injection current; I_{th} is the threshold current ($I_{\mathrm{th}} = (F\beta + (1-\beta))\, N_{\mathrm{th}} eV\alpha/\tau_n$), V_a is the volume of the active region e is the electron charge and N_{th}($N_{\mathrm{th}} = N_o + 1/\Gamma g_n \tau_p$) is the threshold carrier density. $\Delta\omega$ is the angular frequency detuning between laser I and laser II. $\tau_{\mathrm{inj}} = D/c$ is the injection delay, where D is the distance between laser I and laser II, c is the speed of light in free space. $\tau_{\mathrm{in}} = 2nL/c$ is the round-trip time in of the laser cavity, where L is the cavity length and n is group refractive index. The mutually-coupled optical injection into the laser I and laser II is controlled by the injection fraction, κ_{inj}, which is related to the injection parameter [25]. Sinusoidal direct current modulation of the lasers included in (2) is characterised by a modulation frequency, f_{m1} or f_{m2}, for the laser I and laser II, and the corresponding depth of modulation h_{m}. The values of the nano-lasers device parameters used in the simulations are provided in Table 1.

Attention is drawn to the fact that an increase of spontaneous emission via the Purcell factor, F or the spontaneous emission coupling factor β may lead to a change in the laser threshold current [15]. This has been taken into account in our previous analysis [17]. Zero cross-talk behaviors can also be found when F is equal or great than 1 and β is 0.1. However if use is made of conventional values of these parameters, i.e. $F = 1$ and $\beta = 10^{-4}$, zero cross-talk behavior is not observed. In that context use is made of just one combination of these parameters, viz., Purcell factor, $F = 14$ and spontaneous emission coupling factor, $\beta = 0.1$. This choice of parameters exemplifies regimes where mutually coupled nano-lasers display remarkable stability even when subject to strong coupling [17]. The remaining device parameters are also chosen to be the same for both lasers. Modulation is applied over timescales ranging from 2 ns to 12 ns.

3. Identification of Zero-Cross-Talk Regimes

The purpose of this paper is to demonstrate that dually modulated mutually-coupled nano-lasers can be operated in so-called zero cross-talk regimes where the dynamics of one or both nano-lasers is independent of the dynamics of the other nano-laser. It has been shown in previous work that nano-lasers with significant Purcell cavity-enhanced spontaneous emission factors, F, and large spontaneous emission coupling factor β, are robust to external optical perturbations including optical injection [25], conventional optical feedback [32] and phase-conjugate optical feedback [33]. Such robustness to external stimuli has also been revealed in considerations of the dynamics of mutually-coupled nano-lasers [17] as well as in dually modulated mutually-coupled nano-lasers [18]. In the case of modulation, the robustness manifests itself as regimes of zero cross-talk whose existence has been noted in previous work [34]. In the calculation we firstly find the stable state of the mutually-coupled nano-lasers, that is, the region of injection strength which makes the lasers

TABLE 1
Nano-Laser Device Parameters

Wavelength	λ	1591 nm	[12]
Cavity length	L	1.39 μs	[12]
Volume of active region	V_b	3.96×10^{-19} m^3	[12]
Group refractive index	n	3.4	[12]
Round-trip time in inner cavity	τ_{in}	0.032 μs	[12]
Photon lifetime	τ_p	0.36 ps	[12]
Carrier lifetime	τ_n	1 ns	[30]
Differential gain	G_n	1.65×10^{-12} m^{-3}/s	[12]
Mode confinement factor	Γ	0.645	[12]
Line-width enhancement factor	α	5	[31]
Transparency carrier density	N_0	1.1×10^{24} m^{-3}	[30]
Normalized injection current	j	2–10	
Modulation frequency	f_m	0–70 GHz	
Modulation depth	h_m	0–0.8	
Coupling delay/ distance	τ_{inj} / D	0.05 ns/0.015 m	
Cavity Purcell factor	F	14	
Spontaneous emission coupling	β	0.1	
Injection fraction	κ_{inj}	$0-0.6 \times 10^{-3}$	

stable output. Then we apply the modulation to the two nano-lasers. Here it is first established that two kinds of zero cross-talk regime may arise viz. unidirectional and bi-directional isolated zero cross-talk. Then in Section 4 the direct current modulation properties of dually modulated mutually-coupled nano-lasers in these two regimes are considered.

3.1. Unidirectionally-Isolated Zero Cross-Talk

Here operating conditions are identified in which the response of one nano-laser is isolated from that of the other nano-laser but not vice versa. This is termed unidirectional-isolated zero cross-talk. Fig. 2 gives a typical example where nano-laser I is modulated at 50 GHz whilst nano-laser II is modulated at 20 GHz. In Fig. 2(a) it is apparent in the FFT of the photon density time-series that the dynamics of nano-laser I is affected by both modulation frequencies. On the other hand, from Fig. 2(b) it is clear that the dynamics of nano-laser II is influenced only by its own modulation frequency of 20 GHz.

Since all parameters are identical for both nanolasers there should be no asymmetry in the response of the lasers. Indeed in our calculation we observed that with all other parameters fixed the behavior is determined by the relative modulation frequencies. Thus,for example, if we exchange nanolaser I and nanolaser II their responses are exchanged: that is in Fig. 2. nanolaser I will show its own modulation frequency 20 GHz whilst nanolaser II will show both its own modulation frequency 50 GHz and the coupled laser's modulation frequency 20 GHz.

Such unidirectional-isolated behaviour is found to persist for bias currents below 4 I_{th} whilst relatively small values of the modulation depth – up to about 0.3 and relatively strong coupling strengths say $\kappa_{inj} = 0.5 \times 10^{-3}$.

3.2. Bi-Directionally-Isolated Zero Cross-Talk

A stronger form of zero cross-talk arises where both nano-lasers operate independently of each other and which is therefore termed bi-directional-isolated zero cross-talk. Such operation is shown

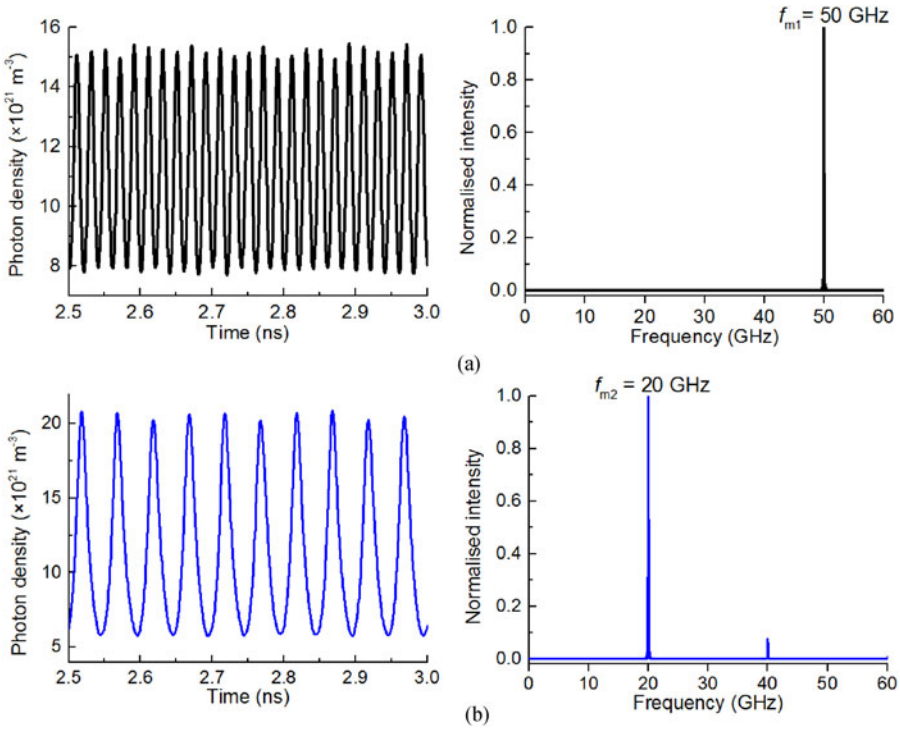

Fig. 2. Photon density time series and FFT for $I_{\mathrm{I}} = I_{\mathrm{II}} = 2I_{\mathrm{th}}$, $h_m = 0.2$ and $\kappa_{\mathrm{inj}} = 0.5 \times 10^{-3}$. (a) nano-laser I with f_{m1} 50 GHz, (b) nano-laser II with f_{m2} 20 GHz.

to be achievable for a range of experimentally adjustable parameters. Specifically as the bias current is increased bi-directional-isolated zero cross-talk may be obtained over a larger range of modulation depths. Similarly the range of coupling strengths over which bi-directional-isolated zero cross-talk is maintained enlarges with increasing modulation depth.

Calculations, for weak injection coupling $\kappa_{\mathrm{inj}} = 0.1 \times 10^{-3}$, but with a bias current of 6 I_{th}, are displayed in Fig. 3. It is observed in Fig. 3, that both nano-lasers exhibit either a single frequency response seen in Fig. 3(a) or possible harmonics of their relevant modulation frequency as given in Fig. 3(b).

4. Modulation Response in Zero Cross-Talk Regimes

Having identified two general classes of zero cross-talk modulation regimes, attention is now focussed on the direct current modulation response of dually modulated nano-lasers in these regimes.

The modulation response index, η defines as:

$$\eta = \frac{S_{\mathrm{max}}(t) - S_{\mathrm{min}}(t)}{S_{\mathrm{mean}}(t)} \tag{6}$$

where $S(t)$ is photon density of nanolaser in modulation. By altering modulation frequency, f_{m1} or f_{m2}, the corresponding response index values are obtained. In our previous work [24], [25], the modulated nano-laser displays a strong response compared with the conventional laser, and the modulation bandwidth which is the frequency f_{m} at $\eta = -3$ dB is predicted to reach 90 GHz for an optical injected nanolaser [25].

Since zero cross-talk displays a range of interactions depending on bias currents, injection coupling and modulation depth, in this section, we display the modulation response both in the

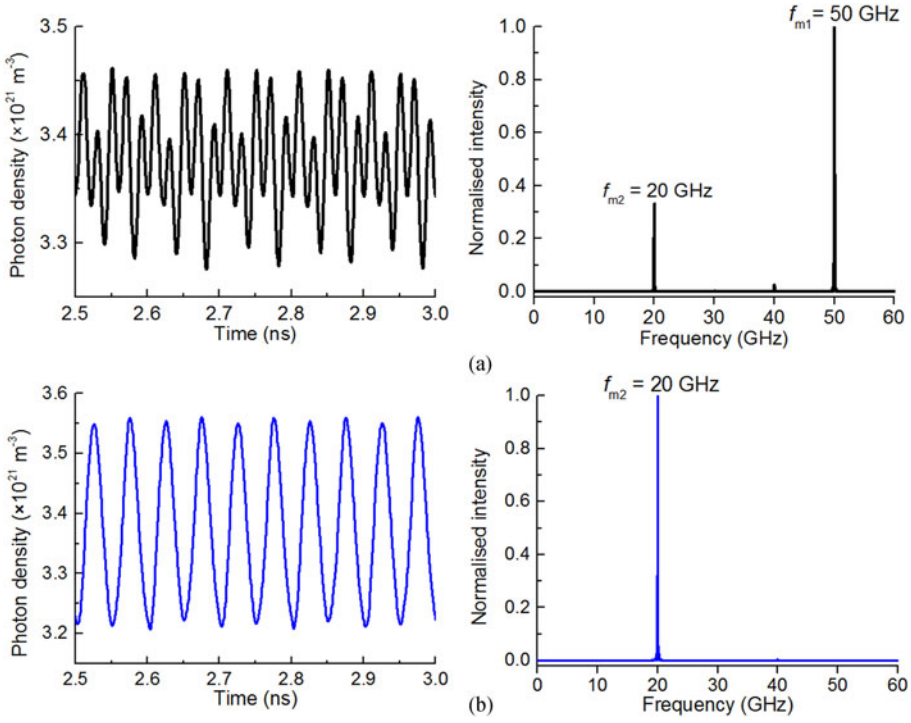

Fig. 3. Photon density time series and FFT at $I_I = I_{II} = 6I_{th}$, $h_m = 0.6$ and $\kappa_{inj} = 0.1 \times 10^{-3}$. (a) nano-laser I with f_{m1} 50 GHz, (b) nano-laser II with f_{m2} 20 GHz.

unidirectional and bi-directional isolated regime as a function of bias currents. We then focus on the modulation bandwidth in the bi-directional isolated regime only.

4.1. Unidirectional-Isolated Regime

In the unidirectional-isolated zero cross-talk regime, the dynamics of one nano-laser is immune to changes in the dynamics of the other but not vice versa. This property would be expected to translate into unchanging modulation properties of the immune nano-laser when the modulation state of the other laser is changed. This is illustrated in Fig. 4, where we calculate the modulation response index with various combinations of f_{m1} and f_{m2}. Fig. 4(a) shows the influence of laser with lower modulation frequency (laser-I) on the laser with high modulation frequency (laser-II), wherein laser-II displays different modulation indices for $f_{m1} = 20$ GHz and $f_{m1} = 30$ GHz. In the case of relatively higher modulation frequencies for laser-I, $f_{m1} = 50$ GHz and $f_{m1} = 70$ GHz, as shown in Fig. 4(b), the modulation index of laser-II does not change. Our calculations show that it is a generic feature that the laser subject to the lower modulation frequency is immune to the laser subject to the higher modulation frequency.

It is observed in Fig. 4 that the modulation index significantly increases with increasing bias currents. However it is noted that the modulation indices are typically less than -3 dB. In addition, it has already been seen from Fig. 2(a) that the laser subject to the relatively high modulation frequency displays multiple-periodic behaviour. Due to these unfavourable factors more detailed investigation of the modulation response in the unidirectional isolated regime is not pursued further here.

4.2. Bi-Directionally-Isolated Regime

The characteristic of the bi-directional-isolated zero cross-talk regime is that both nano-lasers are immune to each other, i.e., both operate independently. Again, this would be expected to be reflected in the modulation responses of each of the nano-lasers as the modulation state of the

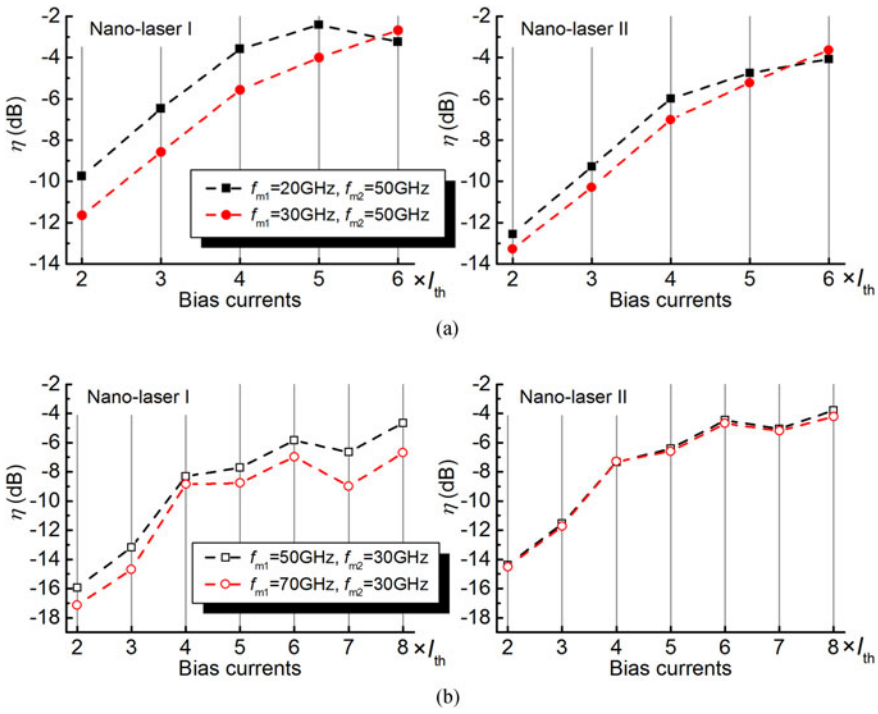

Fig. 4. Modulation response vs. bias currents: (a) laser-I with f_{m1} 20 GHz and 30 GHz, laser-II with f_{m2} 50 GHz, at $h_m = 0.2$ and $\kappa_{inj} = 0.5 \times 10^{-3}$; (b) laser-I with f_{m1} 50 GHz and 70 GHz, laser-II with f_{m2} 30 GHz, at $h_m = 0.1$ and $\kappa_{inj} = 0.5 \times 10^{-3}$ (a) $f_{m1} < f_{m2}$, (b) $f_{m1} > f_{m2}$.

other nano-laser is changed. Fig. 5 presents calculations of the bias current dependence of the modulations indices of both lasers when the modulation frequency of laser-I is changed whilst that of laser-II is held fixed. As expected the response of laser-I changes as its modulation frequency is changed but the salient feature of Fig. 5 is that the response of laser-II is unchanged.

To further reveal modulation properties in the bi-directional-isolated regime, in Fig. 6 we show calculations of the modulation index as a function of the modulation frequencies at a number of laser bias currents. Those calculations are also parameterised by an off-set between the modulation frequencies applied to the lasers. Specifically, we examine cases where the difference between f_{m2} and f_{m1} is (a) 5 GHz (b) 10 GHz and (c) 20 GHz when $\kappa_{inj} = 0.1 \times 10^{-3}$ and $h_m = 0.6$. Fig. 6 shows, as usual, that the peak in the response curve moves to higher frequencies and the bandwidth increases when the bias current increases. However, the key feature is that the responses of the lasers are independent. The modulation response of a given laser is solely determined by the modulation frequency and bias current applied to that laser itself. We find that this immunity to coupling laser phenomenon can persist for modulation frequency off-sets of $\Delta f = 30$ GHz. The underlining reason for this behavior is the stability of mutually-coupled nanolasers observed in earlier work [17].

Fig. 7 shows the impact of increased bias current on the modulation bandwidth with $\kappa_{inj} = 0.1 \times 10^{-3}$ (squares) and $\kappa_{inj} = 0.3 \times 10^{-3}$ (circles). It is seen that the direct current modulation bandwidth can reach up to 90 GHz for both weak and strong injection coupling. This indicates that in the bi-directional isolated zero cross-talk regime, the modulated mutually-coupled nano-lasers display a robustness to injection coupling.

5. Discussion

In the above the modulation frequencies are beyond 10GHz. Here, to further display the influences of modulation depth and injection strength on the bi-directional and un-directional isolated

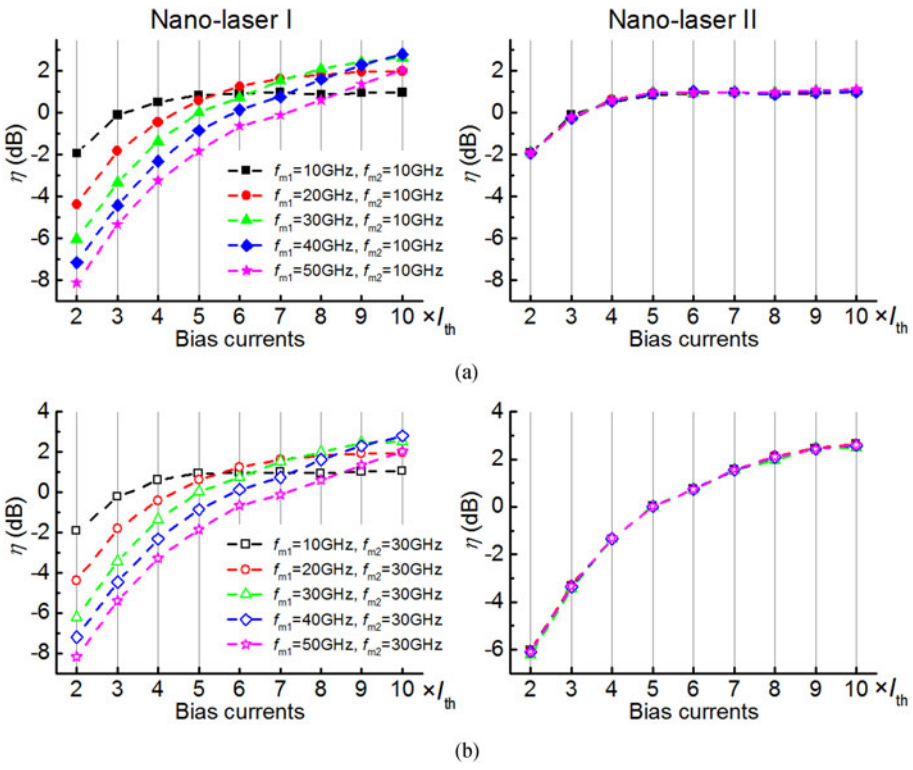

Fig. 5. Modulation response vs. bias currents at $h_m = 0.6$ and $\kappa_{inj} = 0.1 \times 10^{-3}$. Laser-I with f_{m1} from 10 GHz to 50 GHz: (a) laser-II with f_{m2} 10 GHz; (b) laser-II with f_{m2} 30GHz, (a) $f_{m2} = 10$ GHz, (b) $f_{m2} = 30$ GHz.

behaviour, we give some other examples where the modulation frequencies for nanolaser I and nanolaser II are 7 GHz and 3 GHz respectively. Fig. 8 shows the bi-directionally isolated zero cross-talk behaviour, where the bias currents are twice threshold and the modulation depth is 0.6. We notice that even for such modulation depths as 0.1, bi-directionally isolated zero cross-talk can also be observed if injection strength is $\kappa_{inj} = 0.1 \times 10^{-3}$. With other parameters unchanged, if the injection strength increases to say $\kappa_{inj} = 0.3 \times 10^{-3}$, the bi-directionally isolated behavior requires a larger modulation depth: greater than or equal to 0.2.

Our results reveal that strong driving bias currents or deep modulation depth or weak injection coupling strength induces bi-directionally isolated zero cross-talk behaviour, where each of the nanolasers only displays the modulation frequency impressed upon it. Once the injection strength is strong enough, the bi-directionally isolated regime is lost. Then uni-directionally isolated behaviour occurs wherein the nanolaser with the lower modulation frequency simply responds at that lower frequency. In contrast the nanolaser subject to the higher modulation frequency will exhibit responses at both the modulation frequencies impressed upon itself and also that on the other nanolaser. In essence the un-directionally isolated zero cross-talk arises due to the smaller modulation response which arises in the nanolaser subject to the higher modulation frequency as shown in Fig. 6. In consequence the impact of that nanolaser on the nanolaser subject to the lower modulation frequency is small. But, the impact from the coupled nanolaser on the nanolaser subject to the higher modulation frequency is non-negligible.

The basic physical cause of bi-directionally isolated behaviour, is the fact that strong driving bias currents or deep modulation depth or weak injection coupling strength makes each of the modulated mutually-coupled nanolasers independent of each other. However non-linear cross talk will occur if use is made of strong injection coupled power or a very low modulation depth or relatively small bias currents. A more detailed discussion of these aspects is given in [34]. Frequency detuning, the

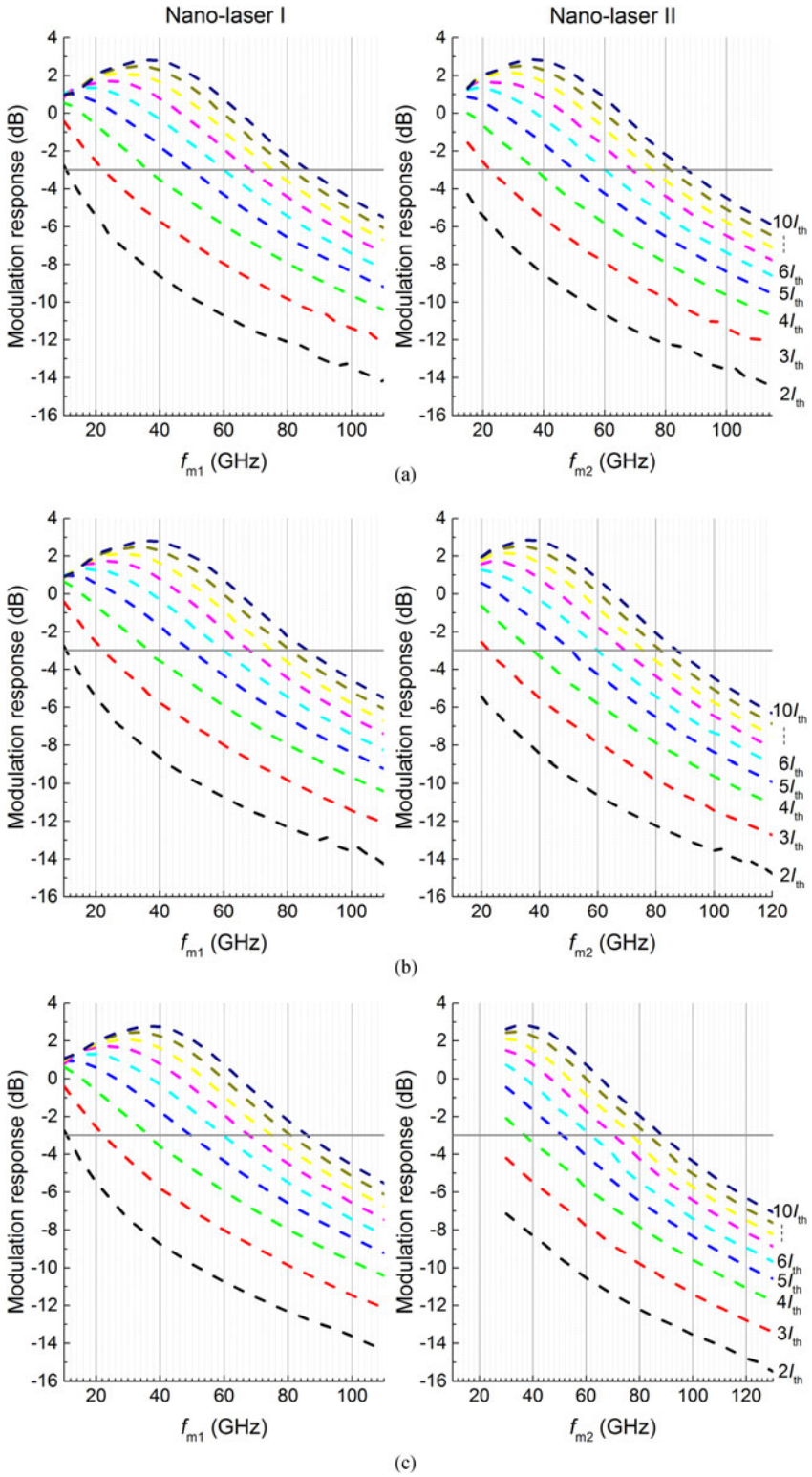

Fig. 6. Modulation response vs. modulation frequencies, at $h_m = 0.6$, $\kappa_{inj} = 0.1 \times 10^{-3}$ for modulation frequency off-set $\Delta f = f_{m2} - f_{m1}$: (a) $\Delta f = 5$ GHz; (b) $\Delta f = 10$ GHz; (c) $\Delta f = 20$ GHz. The curves are for different bias current which, from the bottom up, range from $2I_{th}$ to$10I_{th}$, (a) $\Delta f = 5$ GHz, (b) $\Delta f = 10$ GHz, (c) $\Delta f = 20$ GHz.

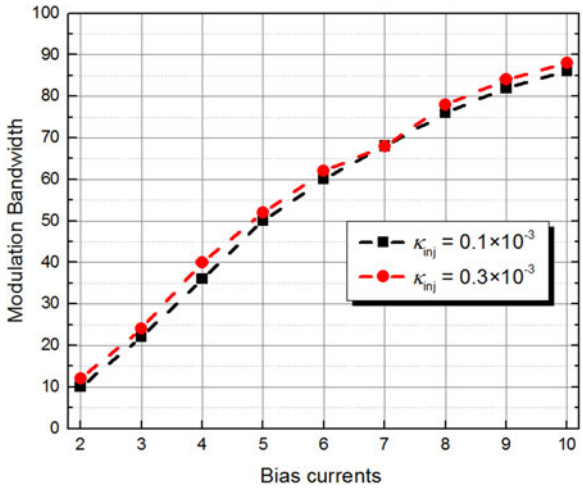

Fig. 7. Modulation bandwidth vs. bias currents for $h_m = 0.6$, at $\kappa_{inj} = 0.1 \times 10^{-3}$ (squares) and $\kappa_{inj} = 0.3 \times 10^{-3}$ (circles).

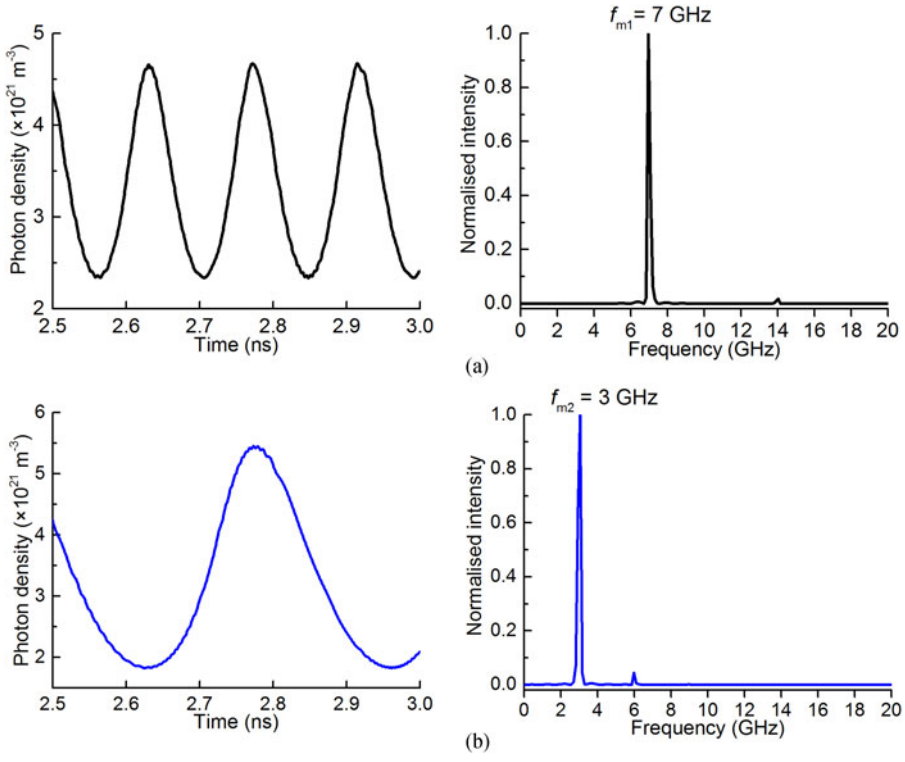

Fig. 8. Photon density time series and FFT at $I_I = I_{II} = 2I_{th}$, $h_m = 0.6$ and $\kappa_{inj} = 0.1 \times 10^{-3}$. (a) nano-laser I with f_{m1} 7 GHz, (b) nano-laser II with f_{m2} 3 GHz.

distance between two lasers and bias current differentials will significantly influence the dynamics of nano-lasers, that is, un-directional isolated zero cross-talk behavior will be replaced by nonlinear behaviors. On the other hand, however, at high bias currents and when the modulation depth is relatively large, bidirectional zero cross-talk is robust to changes in the frequency detuning, the distance between the lasers and bias current differentials.

6. Conclusion

It has been demonstrated that mutually-coupled nano-lasers can be configured such that one or both may be directly modulated independently. A wide range of operating conditions offers access to the requisite bi-directional-isolated zero cross-talk regime wherein the dynamics of both lasers is immune to the dynamics of the other. The configuration is shown to offer the potential for large modulation bandwidths. The capability for effecting such dynamical isolation between the lasers augers well for such a system of mutually-coupled nano-lasers to be utilised in photonic integrated circuits [14].

References

[1] M. B. Spencer and W. E. Lamb, "Theory of two coupled lasers," *Phys. Rev. A*, vol. 5, no. 2, pp. 893–898, Feb. 1972.
[2] A. Hohl, A. Gavriledes, T. Ereux, and V. Kovanis, "Localized synchronization for two delay-coupled semiconductor lasers," *Phys. Rev. Lett.*, vol. 78, pp. 4745–4748, Jun. 1997.
[3] A. Hohl, A. Gavriledes, T. Erneux, and V. Kovanis, "Quasiperiodic synchroniszation for two delay-coupled semiconductor lasers," *Phys. Rev A*, vol. 59, pp. 3941–3949, May 1999.
[4] J. Mulet, C. Mirasso, T. Heil, and I. Fisher, "Synchronization scenario of two distant mutually coupled semiconductor lasers," *J. Opt. B, Quantum Semiclassical Opt.*, vol. 6, pp. 97–105, Nov. 2004.
[5] S. Yanchuk, K. R. Schneider, and L. Recke, "Dynamics of two mutually coupled semiconductor lasers: Instantaneous coupling limit," *Phys. Rev. E*, vol. 69, 2004, Art. no. 056221.
[6] P. Kumar, A. Prasad, and R. Ghosh, "Strange bifurcation and phase-locked dynamics in mutually coupled diode laser systems," *J. Phys. B, Atomic Mol. Opt. Phys.*, vol. 42, no. 14, pp. 145401–145407, Jun. 2009.
[7] Y. Hong, "Flat broadband chaos in mutually coupled VCSELS," *IEEE J. Sel. Topics Quantum Electron.*, vol. 21, no. 6, Nov./Dec. 2015, Art. no. 1801007.
[8] P. Kumar, A. Prasad, and R. Ghosh, "Stable phase-locking of an external-cavity diode laser subjected to external optical injection," *J. Phys. B, Atomic Mol. Opt. Phys.*, vol. 42, Jun. 2008, Art. no. 135402.
[9] E. Clerkin, S. O'Brien, and A. Amann, "Multistabilities and sysmmetry-broken one-color and two-color states in closely coupled single-mode lasers," *Phys. Rev. E.*, vol. 89, Mar. 2014, Art. no. 032919.
[10] E. K. Lau, L. H. Wong, and M. C. Wu, "Enhanced modulation characteristics of optical injection-locked lasers: A tutorial," *IEEE J. Sel. Topics Quantum Electron.*, vol. 15, no. 3, pp. 618–633, May/Jun. 2009.
[11] C. Sun *et al.*, "Modulation characteristics enhancement of monolithically Integrated laser diodes under mutual injection locking," *IEEE J. Sel. Topics Quantum Electron.*, vol. 21, no. 6, Nov./Dec. 2015, Art. no. 1802008.
[12] K. Ding, M. T. Hill, Z. C. Liu, L. J. Yin, P. J. van Veldhoven, and C. Z. Ning, "Record performance of electrical injection subwavelength metallic-cavity semiconductor lasers at room temperature," *Opt. Exp.*, vol. 21, no. 4, pp. 4728–4733, Feb. 2013.
[13] A. V. Maslov and C. Z. Ning, "Size reduction of a semiconductor nanowire laser by using metal coating," *Proc. SPIE.*, vol. 6468, 2007, Art. no. 646801.
[14] Q. Gu and Y. Fainman, *Semiconductor Nanolasers*. Cambridge, U.K.: Cambridge Univ. Press, 2017.
[15] T. Suhr, N. Gregersen, M. Lorke, and J. Mφrk, "Modulation response of quantum dot nanolight-emitting-diodes exploiting purcell-enhanced spontaneous emssion," *Appl. Phys. Lett.*, vol. 98, May 2011, Art. no. 211109.
[16] H. Gao, A. Fu, S. C. Andrews, and P. Yang, "Cleaved-coupled nanowire lasers," *Proc. Nat. Acad. Sci.*, vol. 110, no. 3, pp. 865–869, Jan. 2013.
[17] H. Han and K. A. Shore, "Dynamics and stability of mutually coupled nano-lasers," *IEEE J. Quantum Electron.*, vol. 52, no. 11, Nov. 2016, Art. no. 2000306.
[18] H. Han and K. A. Shore, "Noise-robust high-frequency small-signal oscillations in mutually coupled nano-lasers," *Photonics Res.*, to be published.
[19] A. M. Yacomotii, S. Haddadi, and S. Barbay, "Self-pulsing nanocavity laser," *Phys. Rev. A*, vol. 87, Jul. 2013, Art. no. 041804.
[20] M. Lorke, T. Suhr, N. Gregersen, and J. Mφrk, "Theory of nanolaser devices: Rate equation analysis versus microscopic theory," *Phys. Rev. B*, vol. 87, May 2013, Art. no. 205310.
[21] K. Ding and C. Z. Ning, "Metallic sub-wavelength-cavity semiconductor nanolasers," *Light, Sci. Appl.*, vol. 1, no. 7, Jul. 2012, Art. no. e20.
[22] M. Marconi, J. Javaloyes, F. Raineri, J. A. Levenson, and A. M. Yacomotti, "Asymmetric mode scattering in strongly coupled photonic crystal nanolasers," *Opt. Lett.*, vol. 41, no. 24, pp. 5628–56231, Dec. 2016.
[23] P. Kumar and F. Grillot, "Control of dynamical instability in semiconductor quantum nanostructures diode lasers: Role of phase- amplitude coupling," *Eur. Phys. J. Spec. Topics*, vol. 222, no. 3, pp. 813–820, Jul. 2013.
[24] Z. A. Sattar and K. A. Shore, "Analysis of the direct modulation response of nanowire lasers," *J. Lightw. Technol.*, vol. 33, no. 14, pp. 3028–3033, Jul. 2015.
[25] Z. A. Sattar, N. A. Kamel, and K. A. Shore, "Optical injection effects in nanolasers," *IEEE J. Quantum Electron.*, vol. 52, no. 2, Feb. 2016, Art. no. 1200108.
[26] R. Aust, T. Kaul, C. Z. Nong, B. Liganau, and K. Ludge, "Modulation response of nanolasers: What rate equation approaches miss," *Opt. Quantum Electron.*, vol. 48, Feb. 2016, Art. no. 109.
[27] K. Ding *et al.*, "Electrical injection continuous wave operation of sub wavelength-metallic-cavity lasers at 260 K," *Appl. Phys. Lett.*, vol. 98, no. 23, Jun. 2011, Art. no. 231108.

[28] K. A. Shore, "Modulation bandwidth of metal-clad semiconductor nanolasers with cavity-enhanced spontaneous emission," *Electron. Lett.*, vol. 46, no. 25, pp. 1688–1689, 2010.
[29] K. Ding, J. O. Diaz, D. Bimberg, and C. Z. Ning, "Modulation bandwidth and energy efficiency of metallic cavity semiconductor nanolasers with inclusion of noise effects," *Laser Photon. Rev.*, vol. 9, no. 5, pp. 488–497, 2015.
[30] L. A. Coldren and S. W. Corzine, *Diode Lasers and Photonic Integrated Circuits.* New York, NY, USA: Wiley, 1995.
[31] S. W. Chang, "Dressed linewidth enhancement factors in small semiconductor lasers," *Opt. Exp.*, vol. 20, no. 15, pp. 16450–16470, Jul. 2012.
[32] Z. A. Sattar and K. A. Shore, "External optical feedback effects in semiconductor nano-lasers," *IEEE J. Sel. Topics Quantum Electron.*, vol. 21, no. 6, Dec. 2015, Art. no. 1800106.
[33] Z. A. Sattar and K. A. Shore, "Phase conjugate feedback effects on nano-lasers," *IEEE J. Quantum Electron.*, vol. 52, no. 4, Apr. 2016, Art. no. 1100108.
[34] H. Han and K. A. Shore, "Modulated mutually coupled nano-lasers," *IEEE J. Quantum Electron.*, vol. 53, no. 2, Apr. 2017, Art. no. 2000208.